

Crypsis in the pelagic realm: evidence from exceptionally preserved fossil fish larvae from the Eocene Stolleklint Clay of Denmark

Supplementary Information

Figure S1

Energy-dispersive X-ray spectroscopic maps

Figure S2

Energy-dispersive X-ray spectroscopic line scan

Figure S3

Selected spectra from energy-dispersive X-ray spectroscopy

Figure S4

Positive TOF-SIMS spectra

Figure S5

Positive ToF-SIMS ion images

Table S1

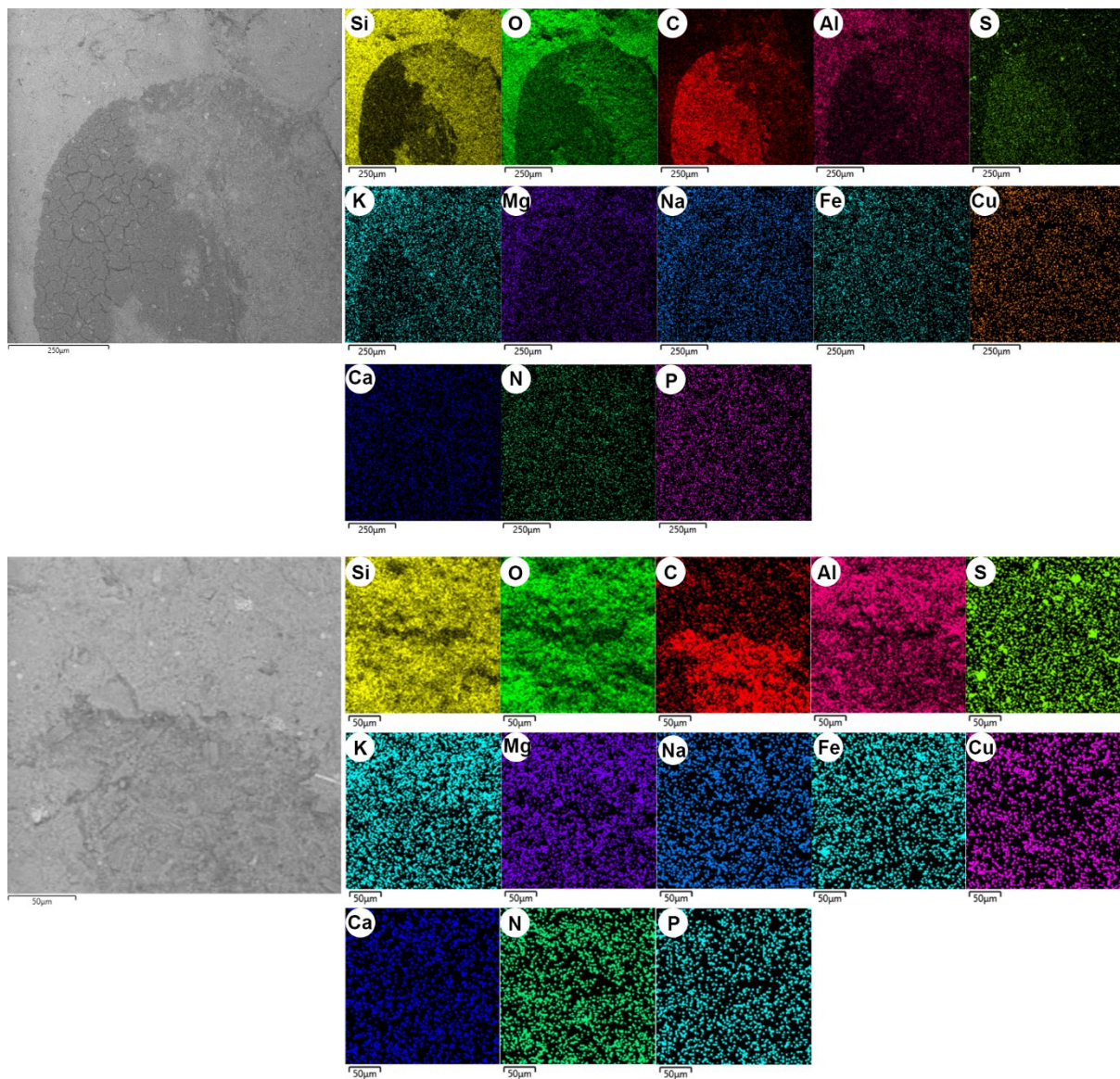
Eumelanin-related ions in the negative-ion spectra (ToF-SIMS)

Table S2

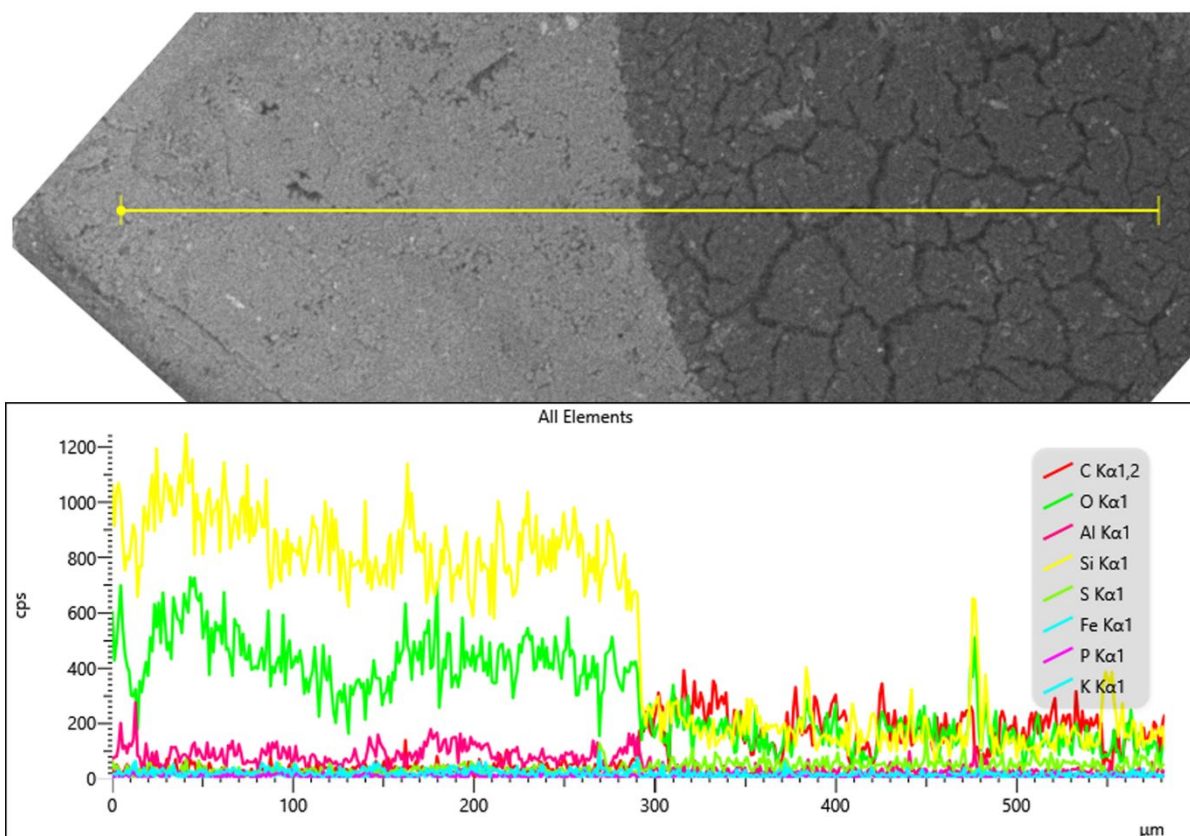
Sediment- and sulfate-related ions in the negative-ion spectra (ToF-SIMS)

Table S3

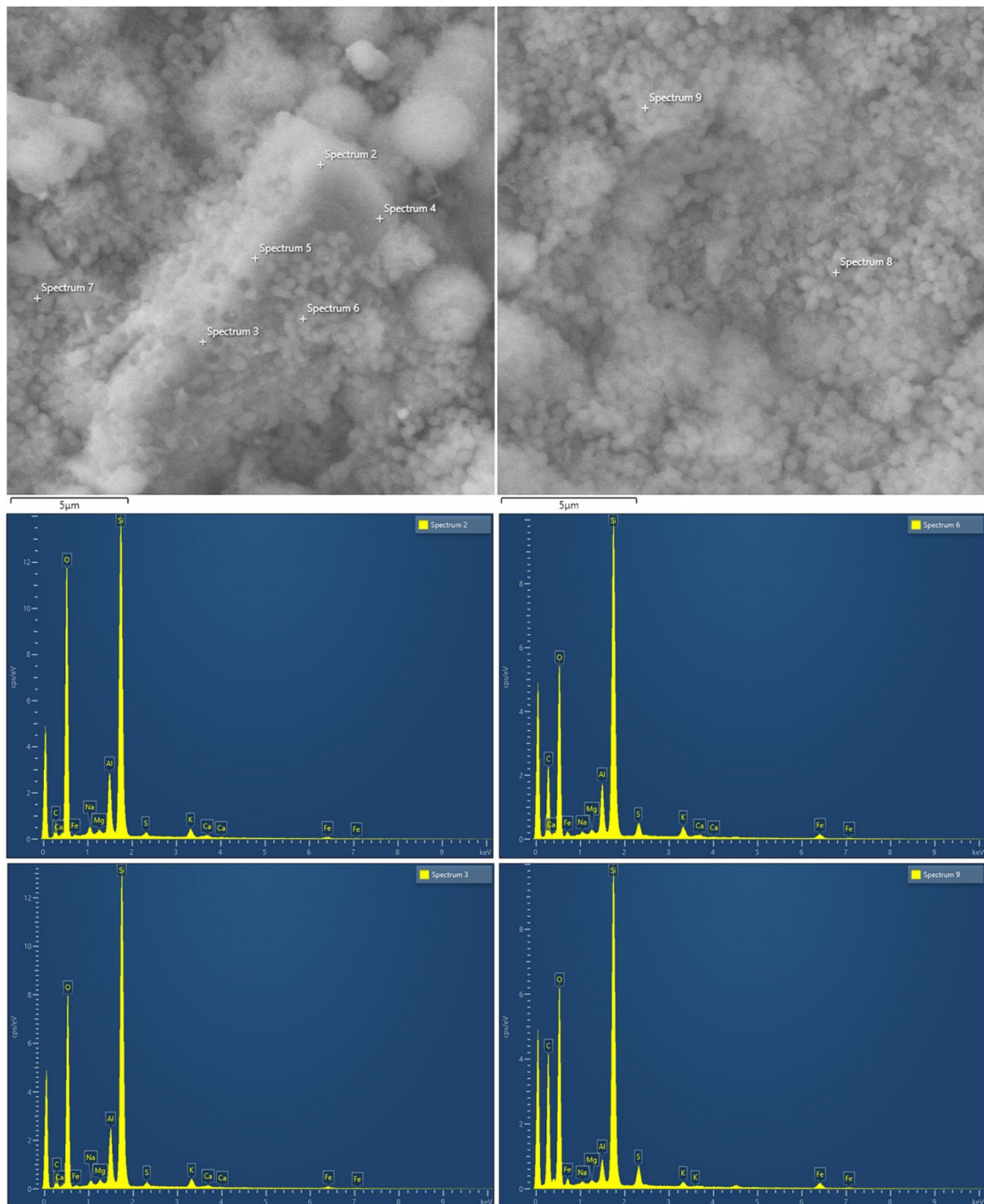
Protein fragment ions in the positive-ion spectra (ToF-SIMS)



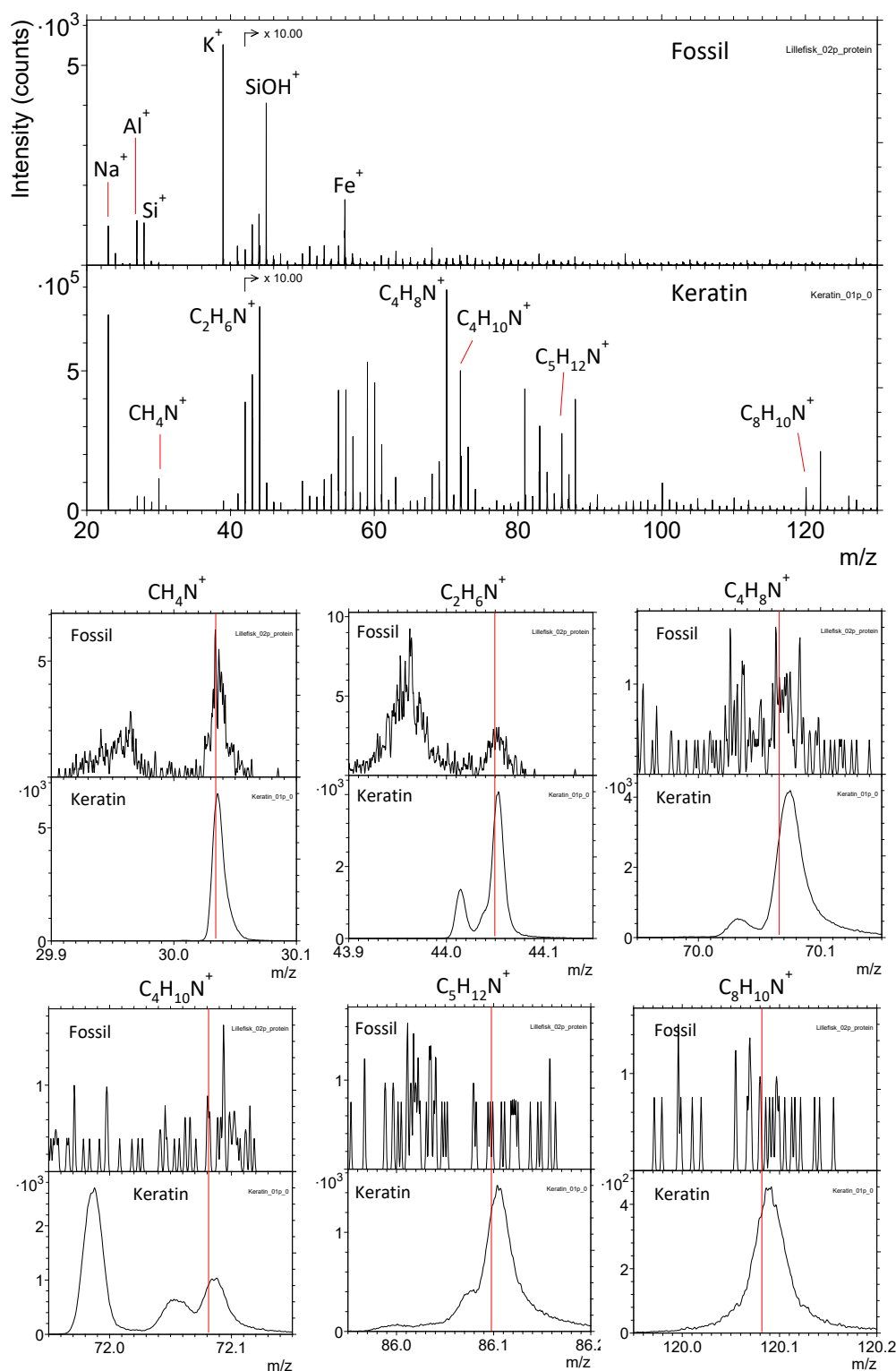
Supplementary Figure S1 Energy-dispersive X-ray spectroscopic maps of the remnant eye (top) and (posterior) peritoneum (bottom) in NHMD 625460. Carbon is prominent in the pigmented areas, whereas silicon and oxygen dominate in the surrounding sediment.



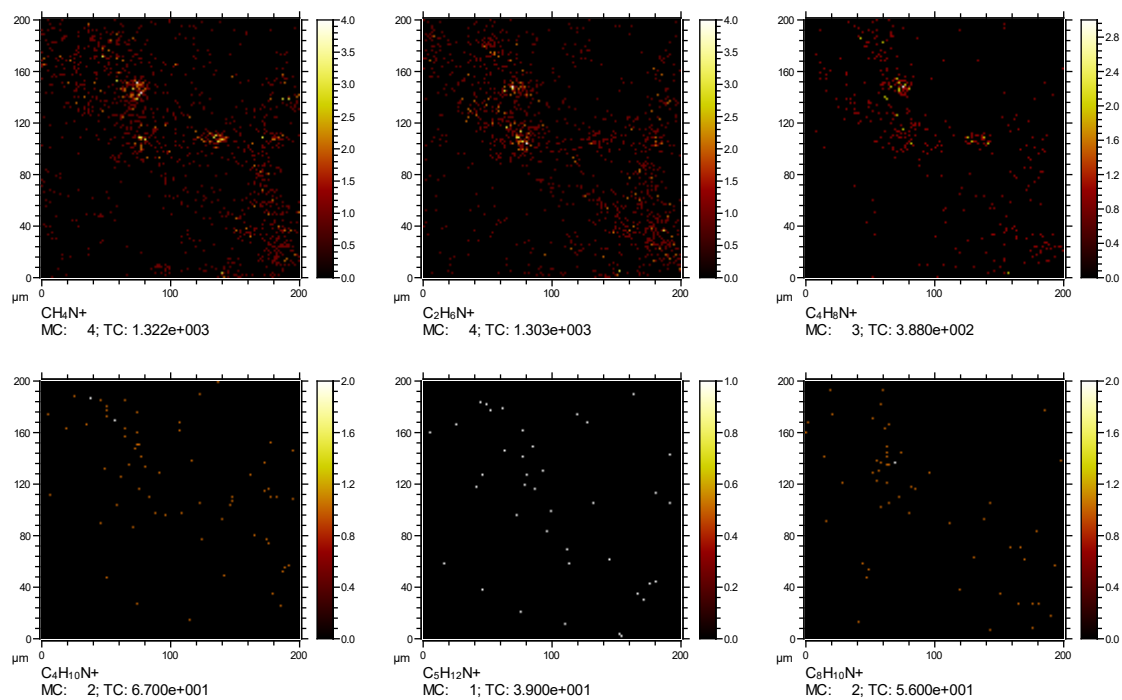
Supplementary Figure S2 Energy-dispersive X-ray spectroscopy across the sediment and remnant eye of NHMD 625460, showing a clear difference in elemental composition between the two substrates.



Supplementary Figure S3 Selected spectra from Energy-dispersive X-ray spectroscopy representing the melanosome-like microbodies (spectra 6 and 9) and the mineral precipitation (spectra 2 and 3) in the posterior part of the peritoneal pigmentation of NHMD 625460. Carbon was more prominent among the microbodies than in the precipitate, which was dominated by oxygen, silicon and aluminium.



Supplementary Figure S4 Positive TOF-SIMS spectra of ROI in the peritoneal trace of NHMD 625460 and a keratin reference. The top panel shows that the fossil spectrum is dominated by sediment-related ions, whereas the keratin spectrum displays strong signal intensity from protein fragment ions (labelled). The lower panels show each of the discussed protein fragment ion peaks separately, revealing weak but significant signal from these ions also in the fossil spectrum. The red lines indicate the theoretical m/z values for each of the specified protein fragment ions.



Supplementary Figure S5 Positive ion images of protein fragment ions in the peritoneal trace of NHMD 625460. The different ions show similar spatial distributions, although the low signal intensity of the weaker fragment ions results in considerable statistical scattering.

Supplementary Table S1 Assignments of eumelanin-related ions in the negative-ion spectra of NHMD 625460.

Ion	Theoretical mass	Observed mass
C4	48.000	48.000
C4H	49.008	49.009
C3N	50.003	50.005
C5	60.000	60.000
C5H	61.008	61.006
C4N	62.003	62.006
C4HN	63.011	63.013
C4H2N/C3N2	64.019/64.006	64.011
C4HO	65.003	65.007
C3NO	65.998	65.998
C6	72.000	71.994
C6H	73.008	73.005
C5N	74.003	74.001
C7	84.000	83.993
C7H	85.008	85.000
C6N	86.003	85.999
C6HN	87.011	87.007
C6H2N/C5N2	88.019/88.006	88.008
C6HO	89.003	89.006
C5NO	89.998	89.994
C8	96.000	95.993
C8H	97.008	96.998
C7N	98.003	97.995
C9	108.000	107.989
C9H	109.008	108.988
C8N	110.003	109.996
C8HN	111.011	111.001
C8H2N/C7N2	112.019/112.006	112.004
C8HO	113.003	113.005
C7NO	113.998	113.998
C10	120.000	119.985
C10H	121.008	120.993
C9N	122.003	121.989
C11	132.000	-
C11H	133.008	132.999
C10N	134.003	133.997
C10HN	135.011	134.991
C10H2N/C9N2	136.019/135.006	135.999
C10HO	137.003	136.999
C9NO	137.998	138.005
C12	144.000	143.984
C12H	145.008	144.984
C11N	146.003	145.984

Supplementary Table S2 Assignments of sediment- and sulfate-related ions in the negative-ion spectra of NHMD 625460.

Ion	Theoretical mass	Observed mass
AlO2	58.971	58.970
SiO2	59.967	59.962
SiHO2	60.975	60.969
SiO3	75.962	75.956
SiHO3	76.969	76.965
FeO2	87.925	87.919
FeO3	103.920	103.912
FeHO3	104.928	104.918
AlSiO4	118.938	118.928
Si2O5	135.928	135.910
Si2HO5	136.936	136.919
SO2	63.962	63.958
PO3	78.959	78.959
SO3	79.957	79.953
HSO3	80.965	80.964
SO4	95.952	95.942
HSO4	96.960	96.950

Supplementary Table S3 Assignments of protein fragment ions in the positive-ion spectra of NHMD 625460.

Ion	Theoretical mass	Observed mass
CH4N	30.034	30.036
C2H6N	44.049	44.052
C4H8N	70.066	70.069
C4H10N	72.081	72.079
C5H12N	86.097	86.100
C8H10N	120.081	120.082